Scaling Behavior of the Longitudinal and Transverse Transport in Quasi One-Dimensional Organic Conductors

M. Dressel, K. Petukhov, B. Salameh, and P. Zornoza
1. Physikalisches Institut, Universität Stuttgart, Pfaffenwaldring 57, D-70550 Stuttgart, Germany

T. Giamarchi
DPMC, University of Geneva, 24 quai Ernest-Ansermet, CH-1211 Geneva, Switzerland
(Dated: February 2, 2008)

We report on dc and microwave experiments of the low-dimensional organic conductors $(TMTSF)_2PF_6$ and $(TMTSF)_2ClO_4$ along the a, b', and c^* directions. In the normal state of $(TMTSF)_2PF_6$ below $T = 70$ K, the dc resistivity follows a power-law with ρ_a and $\rho_{b'}$ proportional to T^2 while $\rho_{c^*} \propto T$. Above $T = 100$ K the exponents extracted from the data for the a and c^* axes are consistent with what is to be expected for a system of coupled one-dimensional chains (Luttinger liquid) and a dimensional crossover at a temperature of about 100 K. The b' axis shows anomalous exponents that could be attributed to a large crossover between these two regimes. The contactless microwave measurements of single crystals along the b'-axis reveal an anomaly between 25 and 55 K which is not understood yet. The organic superconductor $(TMTSF)_2ClO_4$ is more a two-dimensional metal with an anisotropy $\rho_a/\rho_{b'}$ of approximately 2 at all temperatures. Such a low anisotropy is unexpected in view of the transfer integrals. Slight indications to one-dimensionality are found in the temperature dependent transport only above 200 K. Even along the least conducting c^* direction no region with semiconducting behavior is revealed up to room temperature.

PACS numbers: 71.71.Hf, 71.71.Pm, 74.70.Kn, 71.27.+a

I. INTRODUCTION

The properties of quasi one-dimensional conductors are of particular interest from a theoretical point of view, because in one dimension electron-electron interactions lead to a break-down of the Fermi-liquid picture established half a century ago by Lev Landau [1, 2]. A description by a Tomonaga-Luttinger liquid [3, 4] seems to be more appropriate implying a number of very distinct features like spin-charge separation and power-laws in certain quantities [5, 6]. While the theory of one-dimensional electronic systems was put forward by numerous contributions [7, 8, 9, 10, 11] during the last decades, the experimental realization is only tackled since a few years. Attempts in the field of semiconductor quantum wires, edge states and stripe phases in the quantum Hall effect, carbon nanotubes, and rows of metal atoms on vicinal surfaces have been successful to some degree. In particular the quasi one-dimensional organic conductors of the Bechgaard family [12, 13, 14] serve as model systems to test the theoretical predictions. These compounds are charge transfer salts consisting of stacks of the planar organic molecules TMTSF (which stands for tetramethyltetraselenafulvalene) along the a-axis which are separated in c-direction by monovalent anions like PF_6^-, AsF_6^-, ReO_4^-, or ClO_4^-. In b-direction the distance of the stacks is comparable to the van der Waals radii. Most prominent findings are the reduced density of states at the Fermi energy as indicated by photoemission spectroscopy [15], the c-axis transport investigated by pressure dependent dc resistivity [16], the scaling behavior in the optical conductivity [17], the Hall effect [18, 19], and finally indications of spin-charge separation by the similarity in the spin dynamics [20] and thermal conductivity [21] for TMTSF and TMTTF salts although the electronic transport is very much different; for a review see Ref. [22].

Real materials always have a finite coupling between the chains, no matter how anisotropic they are. The question arises whether the Luttinger liquid effects can be observed in quasi one-dimensional systems. The general expectation is that these compounds cross over from Luttinger liquid behavior to a coherent behavior as the temperature or frequency is lowered [23, 24, 25, 26, 27, 28]; the details, however, are still under debate. For a quasi one-dimensional system with coupling $t_c \ll t_b \ll t_a$, the effective dimensionality depends on the energy range of interest: at low temperatures ($k_BT < t_c$) the system is three-dimensional and only at elevated temperatures ($k_BT > t_b$) or high frequencies ($\hbar\omega > t_b$), one-dimensional properties are expected. In the case of the Bechgaard salts, for instance, the transfer integrals are approximately $t_a : t_b : t_c = 250$ meV : 20 meV : 1 meV, so the bare crossover integral should be of the order of 200 K. Although it was initially believed [23] based on NMR data that this scale would be renormalized by interactions down to 20 K, the more recent optical and transport measurements place [16, 17] this scale at about 100 K.

Only very recently attempts were undertaken to describe a system of weakly coupled Luttinger chains and actually focus on the interchain transport [28, 29, 30]. From an experimental point of view, measurements of quasi one-dimensional organic samples in the direction perpendicular to the needle axis are extremely challenging and only very few results on TMTSF salts have been

published [16, 31, 32, 33, 34, 35, 36, 37]. Here we report on temperature dependent dc and contactless microwave measurements of the electrical conductivity in all three directions of $(TMTSF)_2PF_6$ and $(TMTSF)_2ClO_4$.

II. EXPERIMENTAL DETAILS

Single crystals of the Bechgaard salts $(TMTSF)_2X$ are grown by electrochemical methods in an H-type glass cell between room temperature and 0°C. A constant voltage of 1.5 V was applied between platnium electrodes with an area of approximately 3 cm^2. The current through the solution was between 9.2 and 13.4 μA. To reduce the diffusion, a sand barrier can be introduced. After several months we were able to harvest needle-shaped to flake-like single crystals of several millimeters in length and a considerable width (b'-direction) up to 2 mm. Due the triclinic symmetry, b' denotes the projection of the b axis perpendicular to a, and c^* is normal to the ab plane. The dc resistivity of $(TMTSF)_2PF_6$ along the a-axis was measured on needle-shaped samples with a typical dimension of 2 mm × 0.5 mm × 0.1 mm along the a, b', and c^* axes, respectively. The results on the b'-axis conductivity were obtained on a narrow slice cut from a thick crystal perpendicular to the needle axis; the typical dimensions of so-made samples were $a \times b' \times c^* = 0.2$ mm × 1.3 mm × 0.3 mm. Single crystals of $(TMTSF)_2ClO_4$ have about the same size in a and b' directions (they grow even wider since they are more two-dimensional), however, the thickness (c^* axis) rarely exceeds 50 or 60 μm. Due to our advances in achieving large sample geometry, we were able to measure b'-axis resistivity for the first time with basically no influence of the a and c^* contributions and using standard four-probe technique to eliminate the contact resistances. Also for the c^*-axis transport, we were able to apply four contacts, two on each side of the crystal. The contacts were made by evaporating gold pads on the crystal, then 25 μm gold wires were pasted on each pad with a small amount of silver or carbon paint. The $(TMTSF)_2PF_6$ samples were slowly cooled down to avoid cracks and ensure a thermal equilibrium. In the case of $(TMTSF)_2ClO_4$ we conducted experiments in the relaxed state using a slow cooling rate of less than 0.2 K/min. Employing a ^{3}He cryostat, we cooled down below the superconducting transition at $T_c \approx 1.1$ K. In order to reach the quenched state, the crystal were cooled down rapidly from about 50 K with a rate of more than 50 K/min and the data were subsequently recorded on warming up.

Besides dc experiments we investigated the anisotropic transport of $(TMTSF)_2PF_6$ and $(TMTSF)_2ClO_4$ single crystals in all three directions at microwave frequencies. The major advantage of this method is that no contacts have to be applied. They always lead to a current injection which is not well defined; it cannot be avoided that the contact pads required for dc experiments influence the current flow. It is not always clear which part of the bulk material actually carries the current and which part is probed for the voltage drop. Also surface currents may have a large influence in highly anisotropic conductors. In microwave experiments the dielectric response of the entire sample is integrated; admittedly other factors, like the geometry, the depolarization factor or skin effect cause uncertainties.

For measuring the microwave conductivity in a-direction we employed naturally grown needles of typical dimensions of 1 mm × 0.2 mm × 0.2 mm, in the case of $(TMTSF)_2PF_6$-crystals, for instance. Since a needle-like geometry is best also for precise microwave measurements, we again cut a slice ($a \times b' \times c^* =$ 0.2 mm × 1.2 mm × 0.2 mm) from a thick single crystal to measure in b' direction. In order to perform microwave experiments along the c^* axis, we carefully cut a crystal into several pieces (approximately cubes of 0.2 mm corner size) and arranged up to four as a mosaic in such a way that a needle-shaped sample of about 0.2 mm × 0.2 mm × 0.8 mm was obtained [38]. In the case of $(TMTSF)_2ClO_4$ we had to assemble eleven thin pieces on top of each other to obtain a mosaic of $a \times b' \times c^* = 0.15$ mm × 0.2 mm × 0.66 mm [39].

The microwave experiments utilize three different cylindrical copper cavities which resonate in the TE_{011} mode at 24, 33.5, and 60 GHz. They are fed by voltage-driven Gunn oscillators via suitable waveguides and operate in the transmission mode. The coupling is about 10% and done via two holes in the sidewalls. The crystals are positioned in the maximum of the electric field placed onto a quartz substrate (0.07 mm thick) and can be rotated in situ around one axis. The samples were cooled down slowly (0.2 K per minute, to avoid microcracks) from 300 K to 2 K by coupling to the liquid helium bath with the help of low-pressure He exchange gas and by utilizing a regulated heater. Temperatures as low as 0.7 K could be achieved with a special cavity attached to a ^{3}He chamber [40]. The stability is better than 10 mK [38]. By recording the center frequency f and the halfwidth Γ of the resonance curve as a function of temperature and comparing them to the corresponding parameters of an empty cavity (f_0 and Γ_0), the complex electrodynamic properties of the sample, like the surface impedance, the conductivity and the dielectric constant, can be determined via cavity perturbation theory; further details on microwave measurements and the data analysis are summarized in [41]. The microwave experiments on $(TMTSF)_2ClO_4$ using a fast cooling rate of approximately 12 K/min (in order to prevent the tetrahedral anions to order) could not fully achieve the quenched state, but in some runs we still see slight bumps in the resistivity at the ordering temperature of $T_{AO} = 24$ K. Thus we concentrate here on the relaxed state obtained by cooling with less than 0.2 K per minute; in this case the spin-density-wave state does not show up below $T_{SDW} \approx 6$ K [42]. Since for 60 GHz no complete set of data is available and no unexpected fact are found by now, we will disregard these experiments and focus on 24 and 33.5 GHz.

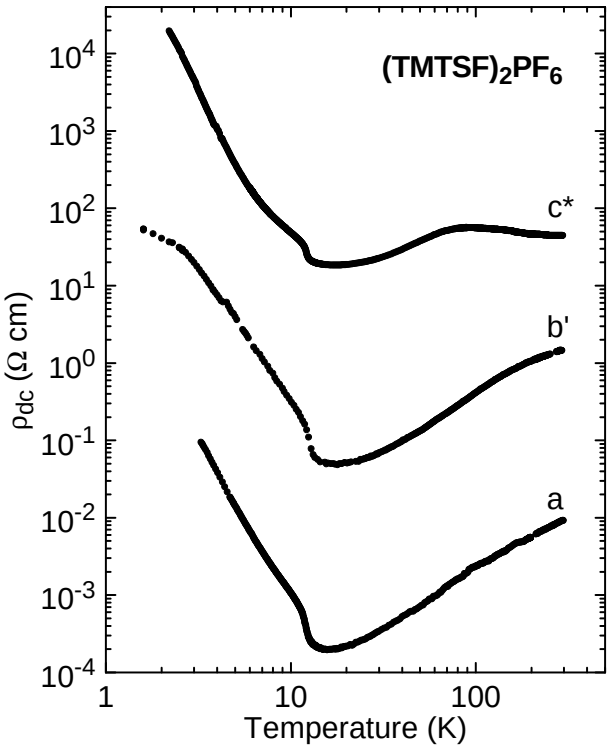

FIG. 1: Overall behavior of the temperature dependent dc resistivity of a $(TMTSF)_2PF_6$ single crystal along the three crystallographic axes a, b', and c^*.

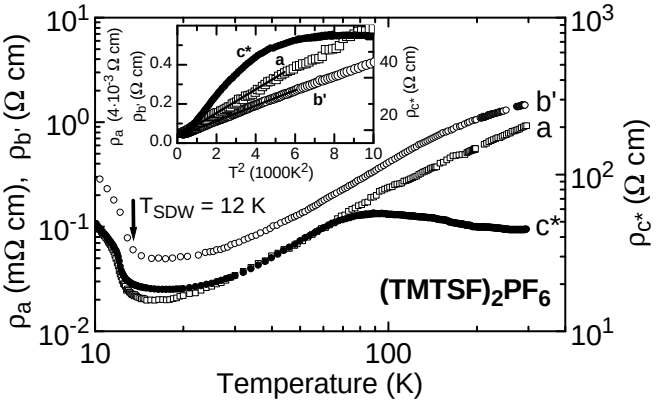

FIG. 2: Temperature dependence of the dc resistivity of $(TMTSF)_2PF_6$ measured along the a (open squares), b' (open circles), and c^* (solid circles) directions. Note the resistivity scales for the three axes. The inset depicts the T^2 dependence of the resistivity below 100 K. Below 65 K, $\rho_{c^*}(T)$ cannot be described by a quadratic dependence; instead it follows a $\rho_{c^*}(T) \propto T$ behavior.

III. RESULTS AND ANALYSIS

A. $(TMTSF)_2PF_6$

1. DC Resistivity

The temperature dependent dc resistivity for all three directions is displayed in Fig. 1. The a-axis transport of $(TMTSF)_2PF_6$ is metallic above $T_{SDW} = 12$ K with a change in slope around 100 K. At high temperatures it can be fitted to a $\rho_a(T) \sim T^{1.3}$ power-law, while for $T <$ 70 K the a-axis resistivity follows the law $\rho_0 + AT^2$, as can be nicely seen in the inset of Fig. 2. For our samples, values of $\rho_0 = 1.1 \times 10^{-4}$ Ωcm and $A = 0.2$ $\mu\Omega$cmK^{-2} are found; the low residual resistivity ρ_0 together with a large resistivity ratio ρ_{300K}/ρ_{20K} indicate a very high crystal quality. The behavior agrees well with previously published data [16, 31, 33, 43, 44].

To our knowledge, there are only two reports [19, 31] on dc measurements of the b'-axis conductivity of $(TMTSF)_2PF_6$ crystals; as a matter of fact both strongly contradict each other. Our findings are in very good agreement with the recent report of G. Mihály *et al.* [19] where the Montgomery method was employed. As plotted in Fig. 2, the resistivity in the intermediate b' direction shows a metal-like behavior; $\rho_{b'}(T)$ decreases almost as steeply as $\rho_a(T)$. The kink in $\rho_{b'}(T)$ shows up at somewhat higher temperatures: it follows the dependence $\rho_{b'}(T) \propto T^{0.84}$ between 300 and 200 K and changes to the $T^{1.63}$ power-law upon further cooling down to 60 K. Below that temperature it can be perfectly described by a quadratic temperature dependence: $\rho_{b'}(T) \propto T^2$ as already found for the a axis (see inset of Fig. 2). In Fig. 3 the ratio of $\rho_{b'}/\rho_a$ is plotted as a function of temperature for both compounds. For $(TMTSF)_2PF_6$ the ratio is basically constant at higher temperatures above 50 K.

For the least conducting direction, $\rho_{c^*}(T)$ increases by about a factor of 1.5 when going from room temperature down to 90 K (Fig. 2). Although no clear power-law is found, the behavior above 100 K may be approximated by $\rho_{c^*}(T) \propto T^{-0.2}$. Below 90 K, $\rho_{c^*}(T)$ falls rapidly before turning upwards again below 15 K due to the spin-density-wave transition. In the temperature range between 35 and 65 K it follows a metallic behavior with $\rho_{c^*}(T) \propto T$. Our findings in the c^* direction are consistent with previous results [16, 19, 31]. The anisotropy ratio ρ_{c^*}/ρ_a (depicted in the inset of Fig. 3) increases continuously by a factor of 100 as the temperature is lowered to T_{SDW} and finally reaches almost 10^5. Again fluctuation effects are seen above the transition.

In order to be able to directly compare our results $\rho(T)$ recorded at ambient pressure with the theoretical models for constant-volume $\rho^{(V)}(T)$ dependence, we converted our experimental data utilizing a procedure as it was previously suggested for $(TMTSF)_2X$ and $(TMTTF)_2X$ salts [13, 35]. The ambient-pressure unit cell at 16 K was taken as reference unit cell; when the temperature T increases, a certain pressure p (depending on the thermal expansion and the compressibility) must be applied (at a given T) in order to restore the reference volume. Since in the metallic phase ρ_a varies by 10% per 1 kbar [16, 19] for all T values above 50 K, the measured resistivity ρ_a is then converted into a constant-volume value $\rho_a^{(V)}$ using

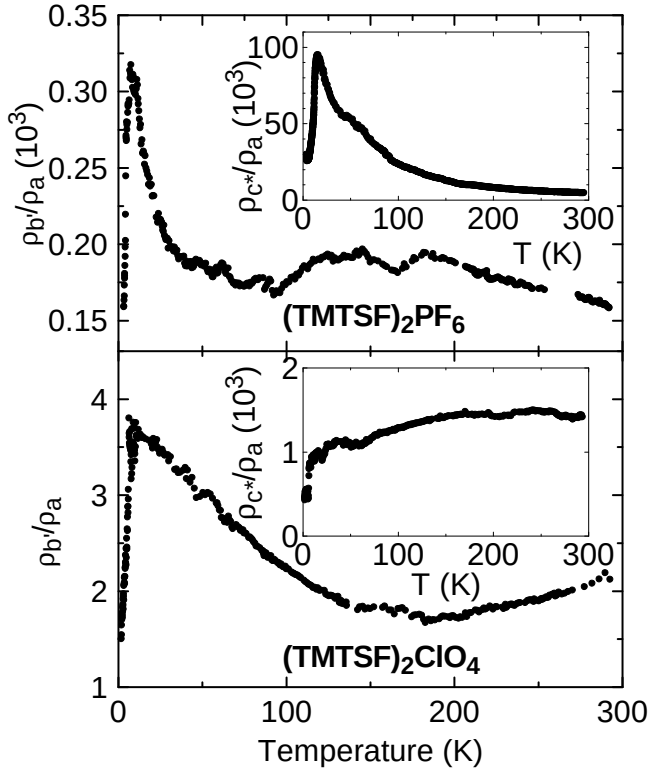

FIG. 3: Temperature dependence of the anisotropy of the dc resistivity $\rho_{b'}/\rho_a$ of the Bechgaard salts. The inset show the temperature dependence of the anisotropy ρ_{c^*}/ρ_a. The upper frame corresponds to $(TMTSF)_2PF_6$ while the data of the lower frame are taken on $(TMTSF)_2ClO_4$.

the expression $\rho_a^{(V)} = \rho_a / \left(1 + p \cdot 0.1\text{kbar}^{-1}\right)$ [45]. The analogous procedure using $10\%\text{kbar}^{-1}$ and the appropriate thermal expansion can be applied for the perpendicular direction in order to get $\rho_{b'}^{(V)}$. It is not clear whether this is also a legitimate procedure with respect to the c^* axis for which a different transport mechanism applies and the variation with pressure is not the same for all temperatures. Hence we restrained ourselves from applying a similar transformation to the c^*-axis data without knowing the exact results.

At low temperature, $T < 50$ K, both the thermal expansion and the pressure coefficient are small [13, 46]. Therefore, the constant-volume temperature dependence of the resistivity does not deviate from the quadratic law observed under constant ambient pressure. In general, the constant-pressure to constant-volume corrections has the consequence that the temperature behavior of the dc resistivity yields reduced power-laws, as can be seen from Fig. 4. Along the chain axis, the constant-volume resistivity follows the power-law $\rho_a^{(V)}(T) \propto T^{0.56}$ from room temperature down to 100 K and lower. The temperature dependence of the transverse b'-axis constant-volume resistivity does not follow a single power-law. Nevertheless, the slope may be approximated by $\rho_{b'}^{(V)}(T) \propto T^{0.24}$ and by $\rho_{b'}^{(V)}(T) \propto T^{0.65}$ in the temperature ranges 200 K $<$

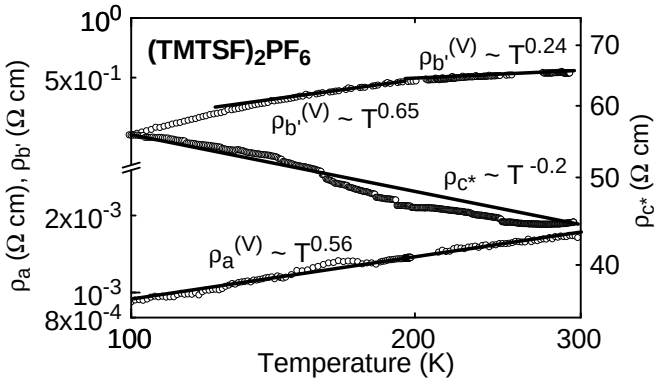

FIG. 4: Log-log presentation of the temperature dependent dc resistivity of $(TMTSF)_2PF_6$ in c^* direction: $\rho_{c^*}(T)$ refers to the right axis. Along the a and b' direction the resistivity normalized to constant volume, $\rho_a^{(V)}(T)$ and $\rho_{b'}^{(V)}(T)$, is plotted corresponding to the left axis. The straight lines indicate to the power-laws.

$T < 300$ K and 150 K $< T <$ 200 K, respectively.

2. *Microwave Experiments*

Since $(TMTSF)_2PF_6$ is highly conducting along the a direction, the data analysis is done in terms of the surface resistance R_S and the surface reactance X_S, assuming that the skin-depth is much smaller than the sample dimension [41]. Our measurements are performed at microwave frequencies for which we expect the Hagen-Rubens limit ($\omega\tau \ll 1$) to be appropriate for our analysis; this was also the case in previous investigations [47]. Indeed, the temperature dependence of the relative change of the halfwidth $\Delta\Gamma/2f_0 = R_S$ and the center frequency $-\Delta f/f_0 = X_S + C$ have the same profile over the wide temperature range, as depicted in Fig. 5a. This is a strong proof that along the a-direction the organic conductor $(TMTSF)_2PF_6$ is in the Hagen-Rubens limit at microwave frequencies, and the surface resistance R_S and the surface reactance X_S (given in units of the free space impedance $Z_0 = 4\pi/c = 377\ \Omega$) have equal absolute values within an additive constant C introduced when the cavity is disassembled in order to mount the sample. Below 12 K the metallic behavior vanishes since $(TMTSF)_2PF_6$ enters the spin-density-wave state. From the surface impedance the calculation of the complex conductivity $\sigma_1 + i\sigma_2$ is straight forward [48]:

$$\sigma_1 = \frac{f_0 R_S X_S}{(R_S^2 + X_S^2)^2}, \quad (1)$$

$$\sigma_2 = \frac{f_0 \left(X_S^2 - R_S^2\right)}{2\left(X_S^2 + R_S^2\right)^2}. \quad (2)$$

The results obtained for $(TMTSF)_2PF_6$ at 33.5 GHz are plotted in Fig. 6. Most obvious, the resistivity ratio $\rho_{300\text{K}}/\rho_{20\text{K}}$ is smaller by a factor of 5 in the microwave

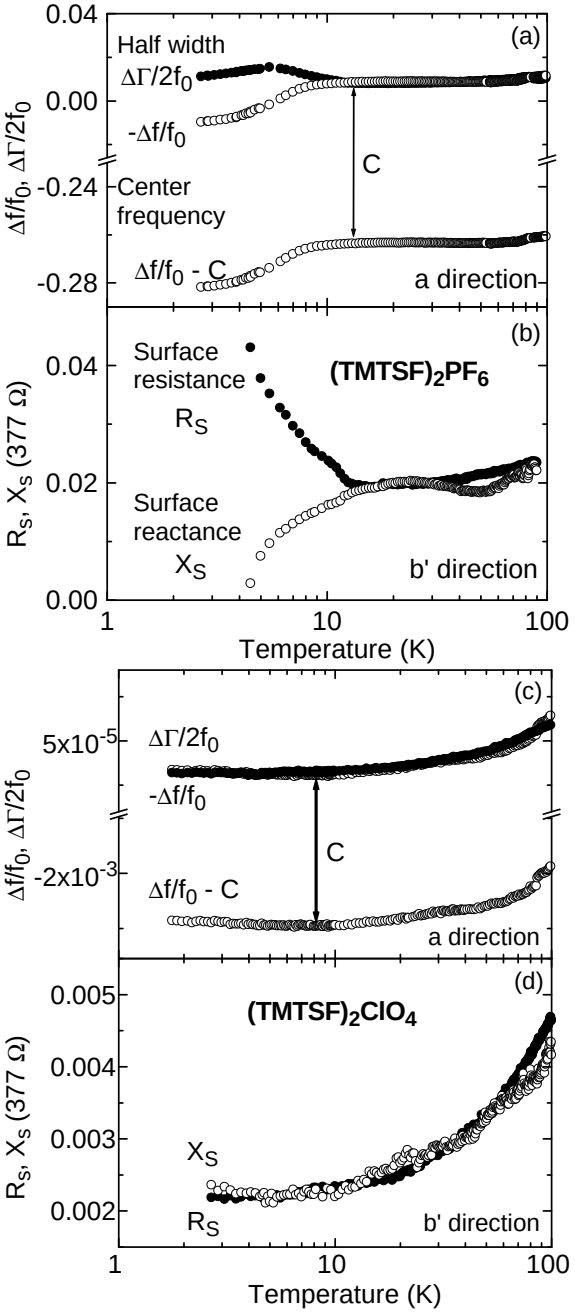

FIG. 5: (a) The shift in center frequency $-\Delta f/f_0$ and the halfwidth $\Delta\Gamma/2f_0$ temperature profiles of a microwave cavity measurement performed at 33 GHz on a $(TMTSF)_2PF_6$ single crystal along the a-axis. By adding a constant value C to the frequency shift $-\Delta f/f_0$ both curves fall on top of each other over a broad temperature range 12 K$< T <$150 K. This implies that the Hagen-Rubens approximation applies at these temperatures: $R_S = \Delta\Gamma/2f_0 \simeq X_S = -\Delta f/f_0$. (b) Also in the b' direction, the surface resistance R_S and the reactance X_S show the same temperature behavior, as expected for a metal in the Hagen-Rubens limit. (c) Accordingly the temperature dependent shift of $-\Delta f/f_0$ and $\Delta\Gamma/2f_0$ of $(TMTSF)_2ClO_4$ along the a direction, and (d) the temperature dependence of the R_S and X_S along the b' direction of $(TMTSF)_2ClO_4$ measured at 24 GHz. Since the crystals remain metallic the Hagen-Rubens condition is always fulfilled.

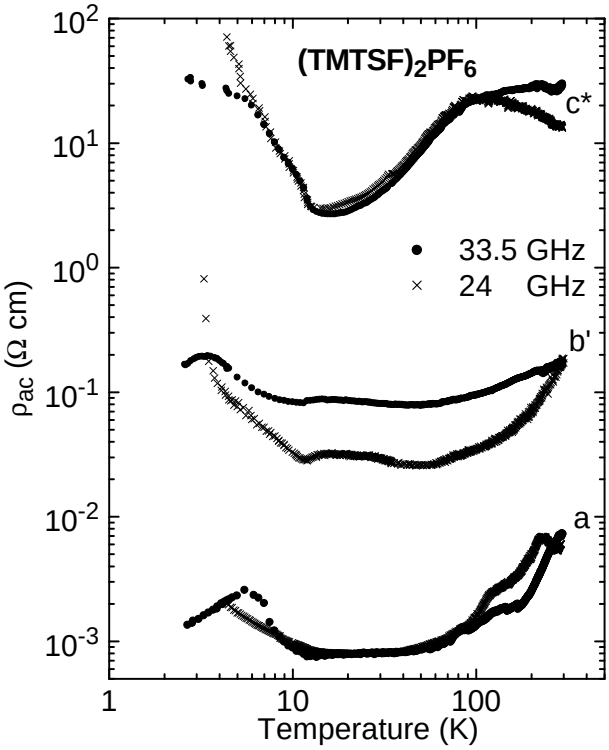

FIG. 6: Temperature dependence of the microwave resistivity of $(TMTSF)_2PF_6$ along the a, b', and c^* crystallographic axes, measured at 24 and 33.5 GHz.

range compared to the dc results; this observation was confirmed by a number of different crystals.

For the analysis of our data measured along the b' direction, i.e. perpendicular to the stacks, we use the same arguments as for the a direction. From the dc conductivity measurements on $(TMTSF)_2PF_6$ we have found that $\rho_{b'}$ is in the order of 0.1–1 Ωcm, which gives us a value for skin depth of 0.1 mm at 33.5 GHz. Thus we expect the system to be in the skin-depth regime along the b' direction, at least in the normal state. Again we find that a good accordance of the surface resistance and surface reactance, as depicted in Fig. 5b. The temperature behavior of the b'-axis conductivity of $(TMTSF)_2PF_6$ probed at 33.5 GHz differs from the dc conductivity along this axis. As can be seen at the enlargement plotted in Fig. 7, the profile of the microwave transport exhibits a change from the metallic behavior to a semiconductor-like behavior for $T < 50$ K. Below a minimum at around 15 to 20 K, $\rho_{b'}(T)$ becomes metal-like on further cooling down to $T_{\rm SDW} = 12$ K, where the SDW transition evidences. This unusual behavior is robust: it has been observed on a large number of different samples and in general coincides with previous results of 16.5 GHz-conductivity measurements on $(TMTSF)_2PF_6$ along the b' direction, which were performed on mosaics [34]. By now it is not clear whether the slight shift to lower temperatures with increasing frequency is significant or not. The Sherbrooke group reports some sample dependence as far as the de-

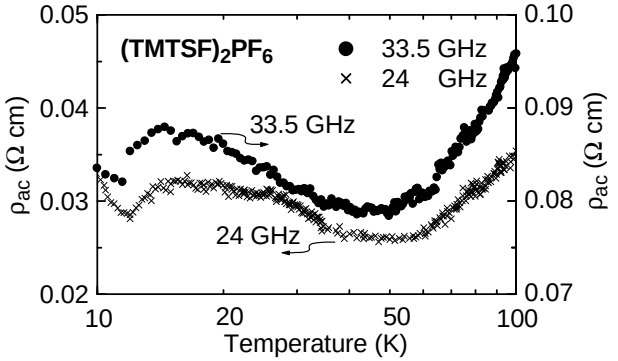

FIG. 7: Enlargement of the temperature dependent microwave resistivity of $(TMTSF)_2PF_6$ along the b' axis.

tailed shape is concerned.

The dc experiments performed along the c^* axis of $(TMTSF)_2PF_6$ yield room temperature values around $\rho_{c^*} = 50$ Ωcm, leading to a skin depth much larger than the sample size. Therefore the data on frequency shift and change of linewidth taken along the c^* direction of $(TMTSF)_2PF_6$ were analyzed according to the depolarization regime [41]. The results obtained on the mosaic assembled from two, three and four cubes coincide perfectly except for the temperature range between 15 and 40 K where the large sample volume with high losses caused an overload of the cavity and we could only use the data of the two-block mosaics [38]. The overall temperature behavior of the c^*-axis microwave conductivity of $(TMTSF)_2PF_6$ shown in Fig. 6 is in good agreement with the dc conductivity data along this direction, except for the temperature region above 80 K, where a slightly semiconducting behavior was observed in the dc results, while the 33 GHz conductivity is almost temperature independent in this temperature region.

Following the measurement procedure and data analysis described above for our 33.5 GHz experiments, we conducted microwave cavity perturbation measurements also for 24 GHz. The results plotted in Fig. 6 confirm our findings in any regard; which is not surprising, since the measurement frequencies are too close to expect a significant frequency dependence. The only point to be noticed is the slightly reduced ratio $\rho(15\text{K})/\rho(300\text{K})$ along the b' direction when going to 33.5 GHz.

B. $(TMTSF)_2ClO_4$

1. DC Resistivity

In Fig. 8 the temperature dependence of the dc transport of $(TMTSF)_2ClO_4$ is plotted for all three directions in the relaxed and the quenched state; no results of all three orientations have previously been published by other groups. K. Murata *et al.* [36] give a room-temperature anisotropy ratio of $\rho_a : \rho_{b'} : \rho_{c^*} \approx 1 : 23 : 900$; their absolute values are in agreement with our findings. A temperature dependence of the a and c^* direction similar to our results was reported by L. Forró *et al.* [37]. Surprisingly we observe a very low anisotropy $\rho_{b'}/\rho_a$, even at room temperature (Fig. 3). Depending on the cooling rate, a clear difference in the low-temperature resistivity $\rho_a(T)$, $\rho_{b'}(T)$ and $\rho_{c^*}(T)$ is found below the anion ordering temperature $T_{\rm AO} = 24$ K. If cooled down slowly with a rate of approximately 0.2 K/min, the relaxed state is reached for which the metallic conductivity continues until the superconducting state is entered at $T_c = 1.1$ K [40]. In all three directions, a significant change in slope $\rho(T)$ can be detected around $T_{\rm AO}$, with only little change in the b' direction. Interestingly, while the resistivity ratio ρ_{c^*}/ρ_a increased strongly by a factor of 50 with decreasing temperature for $(TMTSF)_2PF_6$ (Fig. 3), in the case of $(TMTSF)_2ClO_4$ the anisotropy remains constant down to about 150 K and becomes smaller at lower temperatures.

Along the chains, the resistivity follows a $\rho_a(T) \propto T^{1.5}$ law in the temperature range 25 K $< T <$ 180 K; below 15 K a linear and even sub-linear behavior is found in the relaxed state. Above 200 K the resistivity increases more slowly with temperature, following approximately $T^{0.43}$. The transverse resistivity $\rho_{b'}(T)$ depends linearly

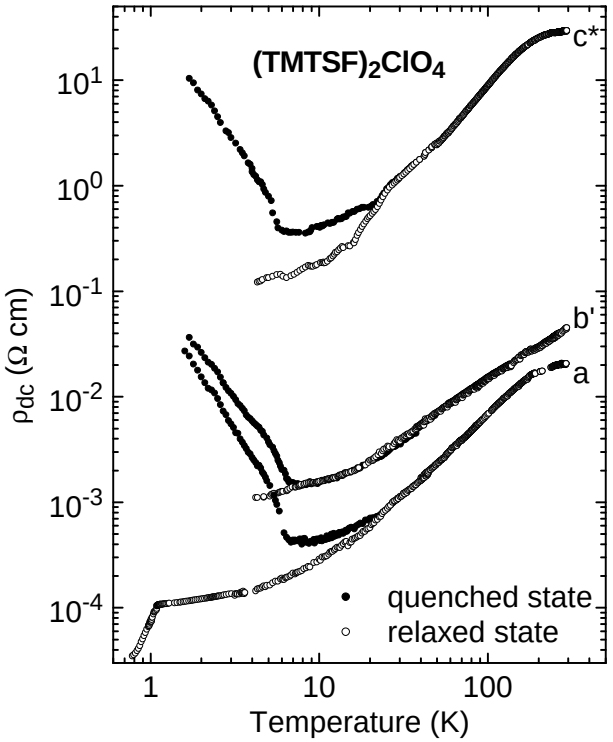

FIG. 8: The dc resistivity of a $(TMTSF)_2ClO_4$ single crystal along the three crystallographic axes a, b', and c^*. The solid points are taken after a rapid cooling faster than 50 K per minute; around 6 K, the crystal enters the spin-density wave state. The open dots correspond to the slow cooled phase which remains metallic and becomes superconducting at $T_c = 1.1$ K.

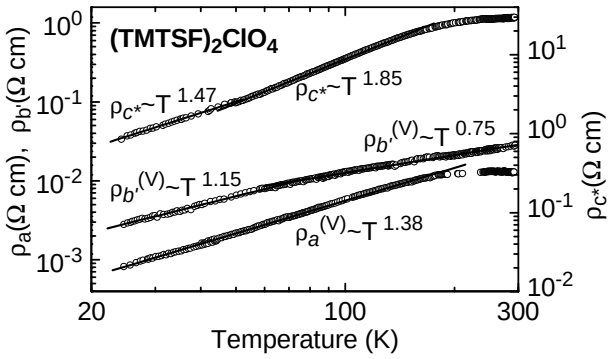

FIG. 9: Temperature dependence of the dc resistivity of $(TMTSF)_2ClO_4$ above the anion ordering temperature T_{AO} in a double logarithmic representation. $\rho_{c^*}(T)$ is the ambient pressure resistivity in c^* direction; along the a and b' direction the data are normalized to constant volume: $\rho_a^{(V)}(T)$ and $\rho_{b'}^{(V)}(T)$. The straight lines correspond to the power-laws as indicated.

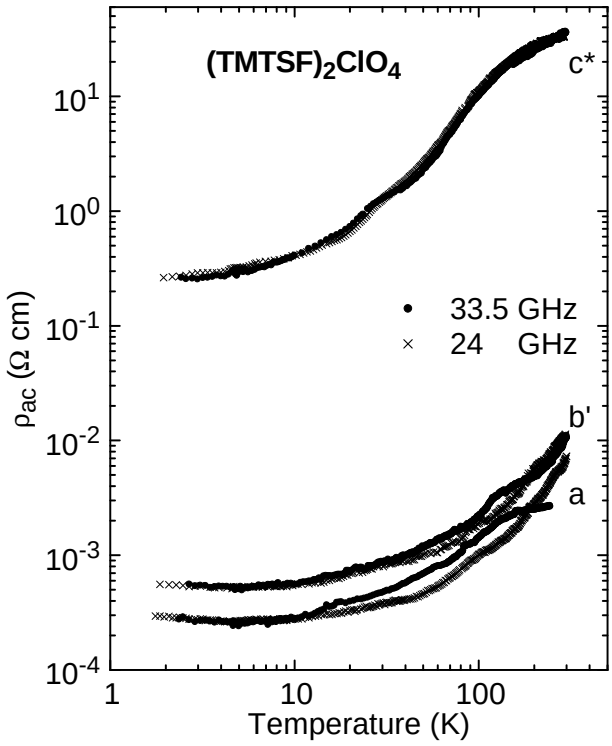

FIG. 10: Temperature dependent microwave resistivity of $(TMTSF)_2ClO_4$ along the a, b', and c^* crystallographic axes, measured at 24 and 33.5 GHz. The data are taken in the relaxed state.

on temperature above 70 K; in the intermediate range (20 K $< T <$ 70 K) a $T^{1.25}$ behavior is observed; the low-temperature resistivity ($T <$ 10 K) can be approximated by $\rho_{b'}(T) \propto T^{0.4}$. A similar slope of $\rho_{c^*}(T) \propto T^{0.5}$ observed for the least-conducting direction; above T_{AO} up to 50 K, the resistivity follows a $T^{1.47}$ power-law, which increases to $T^{1.85}$ for 50 K $< T <$ 150 K. Similar to the a direction, above 200 K $\rho_{c^*}(T)$ exhibits a very slow temperature dependence of $T^{0.34}$.

Following the reasoning given above, we tried to transform the ambient-pressure results to values of the temperature dependent resistivity at constant volume: $\rho_a^{(V)}(T)$, $\rho_{b'}^{(V)}(T)$ and $\rho_{c^*}(T)$ are plotted in Fig. 9. This attempt is hampered by the lack of pressure dependent data on the lattice parameter and the resistivity for $(TMTSF)_2ClO_4$; thus we had to go back and use the transformation procedure applied for $(TMTSF)_2PF_6$. Along the chains we find $\rho_a^{(V)}(T) \propto T^{1.38}$ from the anion ordering temperature $T_{AO} = 24$ K up to almost 200 K; the behavior is temperature independent above. The b'-axis response reveals a change in slope around 75 K for lower temperatures $\rho_{b'}^{(V)}(T) \propto T^{1.15}$ while above the power-law decreases to $T^{0.75}$.

2. *Microwave Experiments*

As far as we know, this is the first microwave investigation performed on $(TMTSF)_2ClO_4$ in all three crystallographic directions. The data along the b' axis shown in [32] are based on the room-temperature anisotropy reported by K. Murata *et al.* [36] and the Hagen-Rubens assumption. The analysis of our microwave data obtained on $(TMTSF)_2ClO_4$ by cavity perturbation technique follows the procedure described above for our measurements on $(TMTSF)_2PF_6$. Along the a and b' axes the skin depth is much smaller than the sample size due to the high conductivity and thus the analysis is done via the surface impedance (Figs. 5c and d). Along the least conducting c^* axis, the quasi-static depolarization regime applies [41].

As seen from Fig. 10, the microwave resistivity exhibits a metallic temperature dependence in all three orientations, although the absolute values are very much different. The temperature dependence of the anisotropy ratios $\rho_{b'}/\rho_a$ and ρ_{c^*}/ρ_a obtained at microwave frequencies is very similar the dc results plotted in Fig. 3. Between the a and b' axes the anisotropy is basically temperature independent and approximately $\rho_{b'}/\rho_a = 2$. The ratio to the c^*-direction is more than three orders of magnitude and decreases linearly by a factor of 10 when the temperature decreases below 150 K. Thus $(TMTSF)_2ClO_4$ resembles a two-dimensional metal much more than a one-dimensional. These findings are supported by optical studies on $(TMTSF)_2ClO_4$ which reveal that the spectral weight of the zero-energy mode is almost isotropic for the a-b plane, while for the c^* direction no Drude contribution was revealed [32].

Along the a and b' axes some of the samples exhibit a T^2 behavior all the way down to 30 K, with no kink observed as known from $(TMTSF)_2PF_6$. The c^* resistivity follows a $\rho_{c^*}(T) \propto T^2$ behavior for $T >$ 30 K with decreasing slope above 130 K. In no temperature regime a semiconducting behavior is found. The anion ordering

at $T_{\rm AO} = 24$ K leads to a slight drop in resistivity with decreasing temperature. For the a and b' directions the resistivity in the range of lower temperatures is close to linear, but does not follow a power-law convincingly.

IV. DISCUSSION

Our results give clear evidence that neither $(TMTSF)_2PF_6$ nor $(TMTSF)_2ClO_4$ can simply be labelled a one-dimensional metal. The coupling in the b' direction between the chains has to be considered. From a theoretical point of view, the transport properties of coupled one-dimensional chains have been investigated [11, 28, 30]. Due to the interactions the effective interchain hopping is renormalized [23], leading to a smaller crossover scale than that for free electrons. A simple expression for this crossover scale is $E^* \propto t\,(t_\perp/t)^{1/(1-\alpha)} = t_\perp\,(t_\perp/t)^{\alpha/(1-\alpha)}$ where α is the single-particle exponent. For commensurate chains a more complex analysis is needed to determine E^* (see e.g. Ref. [29]).

The conductivity parallel [11] to the chains $\sigma_\parallel$ and the conductivity perpendicular [28, 30] to the chains $\sigma_\perp$ were calculated in a system of weakly coupled Luttinger chains. It was found that the interchain hopping is responsible for the metallic character of the $(TMTSF)_2X$ compounds, which would be otherwise Mott insulators. The temperature-dependent transport yields a power-law for the longitudinal and transverse resistivity, respectively:

$$\rho_\parallel(T) \propto (g_{1/4})^2 T^{16K_\rho - 3} \tag{3}$$

$$\rho_\perp(T) \propto T^{1-2\alpha} \tag{4}$$

where $g_{1/4}$ is the coupling constant for the umklapp-scattering process with 1/4 filling, K_ρ is the Luttinger-liquid exponent controlling the decay of all correlation functions ($K_\rho = 1$ corresponds to non-interacting electrons and $K_\rho < 0.25$ is the condition upon which the 1/4 filled umklapp process becomes relevant), and $\alpha = 1/4\,(K_\rho + 1/K_\rho) - 1/2$ is the Fermi-surface exponent. For the frequency-dependent transport the conductivity parallel and perpendicular to the chains is given by power-laws:

$$\sigma_\parallel(\omega) \propto \omega^{16K_\rho - 5} \tag{5}$$

$$\sigma_\perp(\omega) \propto \omega^{2\alpha - 1} \tag{6}$$

Optical experiments on $(TMTSF)_2PF_6$ and $(TMTSF)_2ClO_4$ along the chains [17] yield $K_\rho = 0.23$ in both cases. We now want to see whether we can describe the temperature dependent longitudinal and transverse transport in both compounds consistently. In that respect $(TMTSF)_2PF_6$ and $(TMTSF)_2ClO_4$ have to be distinguished.

A. $(TMTSF)_2PF_6$

Indeed $(TMTSF)_2PF_6$ shows a quite consistent behavior with the above theoretical description, with a crossover scale of about $E^* \approx 100$ K. Although $(TMTSF)_2PF_6$ is highly anisotropic as far as the absolute values of the resistivity are concerned, the temperature dependence below $T \approx 100$ K is the same for the a and b' directions implying a similar transport mechanism. In Fig. 3 the ratios of $\rho_{b'}/\rho_a$ are plotted as a function of temperature. Above 50 K the ratio for $(TMTSF)_2PF_6$ is basically constant and corresponds to the bandstructure anisotropy (this does not hold for the c^*-direction as we will discuss below). Using $4t_a = 1.0$ eV together with measured resistivity gives $(t_a : t_b : t_c) \approx (250 : 10 : 1)$ meV, which is quite close to the anisotropy $(t_a : t_b : t_c) = (250 : 17 : 0.75)$ meV as determined by P. M. Grant by band structure calculations [49]. The increase of $\rho_{b'}/\rho_a$ below 50 K is mainly caused by the transverse resistivity in b' direction which levels off as the spin-density-wave transition at 12 K is approached. It is not clear at this point, however, whether fluctuations are solely responsible for this behavior since they are expected to dominate along the chains. ρ_{c^*}/ρ_a continuously increases by a factor of 50 when going from room temperature to $T_{\rm SDW}$. Since the temperature is always larger than the tunnelling integral along the c^* direction, the conductivity is always incoherent along this axis and measures in fact the tunnelling density of states between the planes. Below 70 K, the dc resistivity of $(TMTSF)_2PF_6$ follows a power-law $\rho_a, \rho_{b'} \propto T^2$, as expected for a Fermi liquid with electron-electron scattering, and $\rho_{c^*} \propto T$. This last behavior is consistent with Eq. (4) when the planes are in a Fermi liquid state since then $\alpha = 0$. From the power-law $\rho_a^{(V)} \propto T^{0.56}$ we found above $T = 100$ K the corresponding Luttinger-liquid exponent can be calculated to be $K_\rho = 0.22$ by using Eq. (3) and $\alpha = 0.69$. This value is in good agreement with the optical data value [17] quoted above. For the c^* direction we observe $\rho_{c^*} \propto T^{-0.2}$ quite consistent with Eq. (4) and the above value of K_ρ (which would lead to $T^{-0.29}$). The interpretation of $\rho_{b'}^{(V)}$ is more complex since no simple power-law was found over the entire temperature range. However a change in the anisotropy behavior is clearly seen to take place above 100 K in Fig. 3 and the fit to a power-law in Fig. 4 shows a downturn of the exponent from 0.65 to 0.24. The data could thus be interpreted as due to a crossover regime between the low-temperature Fermi liquid one and the high-temperature Luttinger liquid. Note that it is reasonable to expect a much larger crossover region for the b'-axis transport, than for the c^* axis given the much higher value of the transfer integral in this direction.

The optical data along the c^* axis [32] is compatible with the above conclusions. The c^*-axis resistivity measured at 24 GHz possess the semiconductor-like behavior ($\mathrm{d}\rho_{c^*}/\mathrm{d}T < 0$) in the high-temperature region

100 K $< T <$ 200 K with the power-law $\rho_{c^*}(T) \propto T^{-0.6}$. From this power-law we obtain $K_\rho = 0.20$, again in reasonable agreement with the other determinations of the Luttinger-liquid exponent. The interpretation of the b'-axis optical data is more complex. Given the above interpretation of the dc transport the system is clearly in the two-dimensional regime for temperatures below 100 K and still in the crossover regime even up to room temperature. Thus an interpretation of the optical data along the b' direction can only be done by using a two dimensional theory for the planes (e.g. along the lines of Ref. [28]). Note that the temperature dependence is quite sensitive to the moderate frequency change, as depicted in Fig. 6. After performing the conversion to constant-volume, we obtain $\rho_{b'}^{(V)}(T) \propto T^{-0.4}$ in the temperature range 20 K$< T <$55 K. This is to be contrasted with the T^2 behavior observed in the dc transport in the same temperature range. The fact that a frequency of an energy corresponding to ~ 1 K gives such a change in the b'-axis conductivity signals a very narrow Drude peak, whose behavior remains clearly to be understood.

B. $(TMTSF)_2ClO_4$

The situation is more complex for $(TMTSF)_2ClO_4$ which obviously exhibits a much more two-dimensional behavior. As can be seen from Fig. 8 the behavior along the a and b' axes is quite similar over the whole temperature range, while the c^* axis remains clearly metallic with a flattening only around 300 K. This suggests that the crossover temperature in the case of $(TMTSF)_2ClO_4$ is higher than 200 K, which means that the dc transport is totally controlled by the two-dimensional physics. Note that the optical data [17] clearly shows for $(TMTSF)_2ClO_4$ the power-law behavior of a Luttinger liquid at high energy, which is consistent with the existence of a crossover scale, but which in that case would be much higher than for $(TMTSF)_2PF_6$. However the dc behavior in the two-dimensional regime is still quite puzzling. From Fig. 3 the anisotropy is approximately temperature independent above 150 K and roughly equal to 2. Although the constant anisotropy is indeed to be expected if the system is in the two-dimensional regime the *value* is quite surprising since it is much *lower* than the ratio that would be expected from the hopping integral, and that would be quite similar to the one actually measured for the case of $(TMTSF)_2PF_6$. The reason for such a low value remains to be understood. The increase of the anisotropy (of about a factor of two until the transition) is reminiscent of the one occurring in $(TMTSF)_2PF_6$ but on a much broader temperature range (100 K instead of less than 50 K for the later). Note also that the exponents for the dc transport are quite different than the ones for $(TMTSF)_2PF_6$. Although $(TMTSF)_2PF_6$ was having the exponents expected for two-dimensional planes in a Fermi-liquid states (T^2 for a and b' axes and T for the incoherent hopping along c^* direction) one finds, as shown in Fig. 9, exponents for the three axis between 1.15 and 1.47.

This difference between $(TMTSF)_2PF_6$ and $(TMTSF)_2ClO_4$, and specially the low value of the anisotropy ration is quite puzzling. In particular it is expected that a universal phase diagram would hold for the organics [12], in which one could go from one chemical compound to the other by applying pressure. This property clearly holds for the various instabilities. It would thus be interesting to make a detailed comparison between $(TMTSF)_2PF_6$ under pressure and $(TMTSF)_2ClO_4$ as far as their transport properties are concerned to check how much of the transport properties of $(TMTSF)_2ClO_4$ can be recovered. Note in particular that it would be unlikely given the amount of pressure to apply to $(TMTSF)_2PF_6$ to change the hopping integrals sufficiently to explain, simply by a modification of the hopping integrals, the low anisotropy ratio observed in $(TMTSF)_2ClO_4$.

V. CONCLUSION

The comparison of the power-laws found in the temperature dependent dc and microwave resistivity of $(TMTSF)_2PF_6$ and $(TMTSF)_2ClO_4$ yields a complex picture. The quadratic behavior found along the chains of $(TMTSF)_2PF_6$ is reduced to $\rho_a(T) \propto T^{1.3}$ above the dimensional crossover around 70 to 100 K; in $(TMTSF)_2PF_6$ we find a maximum in the resistivity $\rho_{c^*}(T)$ around 80 K. The longitudinal and transverse properties in this material are qualitatively consistent from what it to be expected from a system of coupled one-dimensional chains, having a crossover from a Luttinger-liquid at high temperature to a two-dimensional (Fermi liquid) like behavior at low temperatures.

On the contrary, even if optical data shows in $(TMTSF)_2ClO_4$ a one dimensional Luttinger-liquid behavior at high energy, the dc transport shows clearly that below ambient temperature, $(TMTSF)_2ClO_4$ is in a two-dimensional regime. The third direction of $(TMTSF)_2ClO_4$ is metallic in the entire temperature range with some indications to a semiconducting behavior above room temperature, indicating that the crossover temperature should be above ambient temperature. Quite surprisingly the anisotropy ratio, of about 2, is quite low and much lower that what would be expected from the ration of the transfer integrals. Given the idea of a universal phase diagram where change of chemistry would be equivalent to pressure, these measurements suggest a careful comparison between $(TMTSF)_2PF_6$ under pressure and $(TMTSF)_2ClO_4$ to determine the similarities and differences of the two systems.

Acknowledgment

We thank G. Untereiner for the sample growth and preparation. The ^{3}He experiments have been performed

by J. Thoms. The work was supported by the Deutsche Forschungsgemeinschaft (DFG) and by the Swiss National Fund under MANEP and Division II.

[1] L.D. Landau, Sov. Phys. JETP **3**, 920 (1957).
[2] D. Pines and P. Nozières, *The Theory of Quantum Liquids*, Vol. 1 (Addison-Wesley, Reading, 1966).
[3] S. Tomonaga, Prog. Theor. Phys. (Kyoto) **5**, 544 (1950).
[4] J.M. Luttinger, J. Math. Phys. **4**, 1154 (1963).
[5] J. Voit, Rep. Prog. Phys **58**, 977 (1995).
[6] T. Giamarchi, *Quantum Physics in One Dimension* (Oxford University Press, Oxford, 2004).
[7] V. J. Emery, in *Highly Conducting One-Dimensional Solids*, edited by J. T. Devreese *et al.* (Plenum, New York, 1979), p. 327
[8] J. Sólyom, Adv. Phys. **28**, 209 (1979)
[9] F.D.M. Haldene, J. Phys. C **14**, 2585 (1984).
[10] H.J. Schulz, Int. J. Mod. Phys. **5**, 57 (1991).
[11] T. Giamarchi, Phys. Rev. B **33**, 2905 (1991); T. Giamarchi and A.J. Millis, Phys. Rev. B **46**, 9325 (1992); T. Giamarchi, Physica B **230-232**, 975 (1997).
[12] D. Jérome and H. J. Schulz, Adv. Phys. **31**, 299 (1982)
[13] D. Jérome, in *Organic Conductors*, edited by J.-P. Farges (Marcel Dekker, New York, 1994), p. 405.
[14] T. Ishiguro, K. Yamaji, and G. Saito, *Organic Superconductors*, 2nd edition (Springer-Verlag, Berlin, 1998).
[15] B. Dardel, D. Malterre, M. Grioni, P. Weibel, Y. Baer, J. Voit, and D. Jérome, Europhys. Lett. **24**, 687 (1993); F. Zwick, S. Brown, G. Margaritodo, C. Merlic, M. Onellion, J. Voit, and M. Grioni, Phys. Rev. Lett. **79**, 3982 (1997).
[16] J. Moser, M. Gabay, P. Auban-Senzier, D. Jérome, K. Bechgaard, J.M. Fabre, Eur. Phys. J. B **1**, 39 (1998).
[17] M. Dressel, A. Schwartz, G. Grüner, and L. Degiorgi, Phys. Rev. Lett. **77**, 398 (1996); A. Schwarz, M. Dressel, G. Grüner, V. Vescoli, L. Degiorgi, and T. Giamarchi, Phys. Rev. B **58**, 1261 (1998); V. Vescoli, L. Degiorgi, W. Henderson, G. Grüner, K.P. Starkey, and L.K. Montgomery, Science **281**, 1181 (1998).
[18] J. Moser, J.R. Copper, D. Jérome, B. Alavi, S.E. Brown, and K. Bechgaard, Phys. Rev. Lett. **84**, 2674 (2000).
[19] G. Mihály, I. Kézsmárki, F. Zámborszky, and L. Forró, Phys. Rev. Lett. **84**, 2670 (2000).
[20] M. Dumm, A. Loidl, B.W. Fravel, K.P. Starkey, L. Montgomery, and M. Dressel, Phys. Rev. B **61**, 511 (2000); M. Dressel, S. Kirchner, P. Hesse, G. Untereiner, M. Dumm, J. Hemberger, A. Loidl, and L. Montgomery, Synth. Met. **120**, 719 (2001).
[21] T. Lorenz, M. Hofmann, M. Grüninger, A. Freimuth, G.S. Uhrig, M. Dumm, and M. Dressel, Nature **418**, 614 (2002).
[22] M. Dressel, Naturwissenschaften **90**, 337 (2003).
[23] C. Boubonnais, F. Creuzet, D. Jérome, K. Bechgaard, and A. Moradpour, J. Phys. (France) Lett. **45**, L755 (1984).
[24] S. Brazovskii and V. Yakovenko, J. Phys. (France) Lett. **46**, L111 (1985); V.M. Yakovenko, JETP Lett. **56**, 510 (1992).
[25] C. Bourbonnais and L.G. Caron, Int. J. Mod. Phys. B **5**, 1033 (1991).
[26] D.G. Clarke, S.P. Strong, and P.W. Anderson, Phys. Rev. Lett. **72**, 3218 (1994).
[27] H.J. Schulz, in: *Correlated Fermions and Transport in Mesoscopic Systems*, edited by T. Martin *et al.* (Editions Fronìeres, Gif sur Yvette, 1996).
[28] S. Biermann, A. Georges, A. Lichtenstein, and T. Giamarchi, Phys. Rev. Lett. **87**, 276405 (2001).
[29] S. Biermann, A. Georges, T. Giamarchi, and A. Lichtenstein, in: *Strongly Correlated Fermions and Bosons in Low Dimensional Disordered Systems*, edited by I.V. Lerner *et al.* (Kluwer Academic Publishers, Dordrecht, 2002), p. 81; cond-mat/0201542.
[30] A. Lopatin, A. Georges, and T. Giamarchi, Phys. Rev. B **63**, 075109 (2001); A. Georges, T. Giamarchi, and N. Sandler, Phys. Rev. B **61**, 16393 (2000).
[31] C.S. Jacobsen, K. Mortensen, M. Weger, and K. Bechgaard, Solid State Commun. **38**, 423 (1981).
[32] W. Henderson, V. Vescoli, P. Tran, L. Degiorgi and G. Grüner, Europhys. B **11** 365 (1999).
[33] F. Zámborszky, G. Szeghy, G. Abdussalam, L. Forró, and G. Mihály, Phys. Rev. B **60**, 4414 (1999).
[34] P. Fertey, M. Poirier, and P. Batail, Eur. Phys. J. B **10**, 305 (1999).
[35] B. Korin-Hamzič, E. Tafra, M. Basletič, A. Hamzič, G. Untereiner, and M. Dressel, Phys. Rev. B **67**, 014513 (2003).
[36] K. Murata, H. Anzai, G. Saito, K. Kajimura, and T. Ishiguro, J. Phys. Soc. Jpn. **50**, 3529 (1981).
[37] L. Forró, K. Biljakovič, and J.R. Cooper, Phys. Rev. B **29**, 2839 (1984); B. Korin-Hamzič, L. Forró, and J.R. Cooper, Mol. Cryst. Liq. Cryst. **119**, 135 (1985).
[38] K. Petukhov, Ph.D. Thesis, Stuttgart 2003.
[39] P. Zornoza, Master Thesis Stuttgart 2004.
[40] J. Thoms, Ph.D. Thesis, Stuttgart, 2004.
[41] O. Klein, S. Donovan, M. Dressel, and G. Grüner, *Int. J. Infrared and Millimeter Waves*, **14**, 2423 (1993); S. Donovan, O. Klein, M. Dressel, K. Holczer, and G. Grüner, *Int. J. Infrared and Millimeter Waves*, **14**, 2459 (1993); M. Dressel, O. Klein, S. Donovan, and G. Grüner, *Int. J. Infrared and Millimeter Waves*, **14**, 2489 (1993).
[42] The microwave results on the spin-density-wave ground state of $(TMTSF)_2PF_6$ and $(TMTSF)_2ClO_4$ will be presented separately. K. Petukhov and M. Dressel, cond-mat/0408382; P. Zernoza, K. Petukhov, and M. Dressel, *to be published*.
[43] K. Bechgaard, C.S. Jacobsen, K. Mortensen, H.J. Pedersen, and N. Thorup, Solid State Commun. **33**, 1119 (1980).
[44] S. Tomić, J.R. Cooper, W. Kang, D. Jérome, and K. Maki, J. Phys. (Paris) I **1**, 1603 (1991).
[45] Note, that although the value of 25% is reported in Ref. [16], the data actually taken from the graphs of that paper show this value to be around 10%.
[46] B. Gallois, J. Gaultier, T. Lamcharfi, F. Bechtel, and A. Filhol, Synth. Met. **19**, 321 (1987).
[47] S. Donovan, L. Degiorgi, and G. Grüner, Europhys. Lett. **19**, 433 (1992); S. Donovan, M. Dressel, Y. Kim, L. Degiorgi, G. Grüner, and W. Wonneberger, Phys. Rev. B

49, 3363 (1994).
[48] M. Dressel and G. Grüner, *Electrodynamics of Solids* (Cambridge University Press, Cambridge, 2002).
[49] P. M. Grant, Phys. Rev. B **26**, 6888 (1982); P. M. Grant, J. Phys. (Paris) Colloq. **C3**, 847 (1983).